Prediction of Fatigue Crack Propagation Path under Combined Torsional and Axial Loading

K. Tanaka[1] , Y. Akiniwa[1] and S. Wakita[1]

[1]Department of Mechanical Engineering, Nagoya University, Nagoya 464-8603, Japan
E-mail : ktanaka@mech.nagoya-u.ac.jp

ABSTRACT. *A simulation of fatigue crack propagation from a hole or crack under combined axial and torsional loading was conducted on the basis of the maximum tangential stress criterion for determining the crack path. The simulation results were compared with the experimental results obtained from fatigue tests by using thin-walled tubular specimens made of a medium-carbon steel. Fatigue cracks were nucleated at the position of the maximum of the amplitude of the tangential stress around the hole, and propagated straight away from the hole. The path of fatigue crack propagation from a hole or a crack followed the direction perpendicular to the maximum of the range of the tangential stress, $\Delta\sigma^*_{\theta\max}$, near the crack tip calculated from the stress intensity ranges by considering the contact of crack faces. The crack path predicted from the $\Delta\sigma^*_{\theta\max}$ criterion was very close to that calculated from the maximum of the total range of the tangential stress, $\Delta\sigma_{\theta\max}$, calculated by neglecting the crack face contact. The superposition of static mode II shear loading changed slightly the propagation path of a crack propagating under axial tension-compression. This deviation is caused by the generation of cyclic mode II component due to the zigzag shape of a fatigue crack.*

KEYWORDS: Fatigue, Crack propagation, Combined stress, Fracture mechanics, Crack propagation path, Crack face contact, Body force method

INTRODUCTION

Fatigue fracture of several engineering components such as transmission shafts, pipes and suspension coil springs occurs under combined torsional and axial loading. For damage tolerance design, the direction as well as the rate of crack propagation should be predicted from loading conditions.

The maximum tangential stress criterion proposed by Erdogan and Sih for brittle fracture [1] has been used for predicting the propagation path of fatigue cracks of tensile mode by Richard and others [2,3]. The contact of the fatigue fracture surface was not included in their predictions. Tanaka and others [4,5] measured the fatigue crack propagation path from a mode I precrack under cyclic shear loading with the stress ratio $R = -1$. They found that the direction of fatigue crack propagation followed the direction of the maximum of the range of the tangential stress, $\Delta\sigma^*_{\theta\max}$, near the crack tip

determined from the stress intensity factor which was calculated by considering the contacts of crack faces at the minimum load. The stress intensity factor calculated from the actual crack path by using the body force method [6] showed that the mode II stress intensity factor range quickly got close to zero after a small amount of crack extension. The asymmetry of plastic deformation due to cyclic mode II was concluded to be responsible for crack path deviation [7,8].

In the present paper, a simulation of fatigue crack propagation from a hole or a precrack was conducted based on the $\Delta\sigma^*_{\theta\,max}$ criterion under combined mode loading. The effects of load-variation and superposed static shear loading on fatigue crack path were predicted from simulation and compared with the experiments. The tests of fatigue crack propagation were performed on thin-walled tubular specimens made of a medium-carbon steel under cyclic or static torsion with and without static or cyclic axial loading.

SIMULATION PROCEDURE

Crack Propagation Model

For the simulation of fatigue crack propagation, an infinite plate with a precrack under tensile and shear stresses was analyzed as shown in Fig. 1(a). The total length of the precrack was $2c$ (= 1 mm). The origin of the coordinates was taken as the center of a precrack and the angle of crack extension was measured counter clockwise with respect to the horizontal (circumferential) direction. The direction of fatigue crack propagation was predicted by the maximum tangential stress criterion. The stress intensity factor (SIF) value was computed by using the two-dimensional BFM [6]. The curvature effect of thin-walled tubes on the stress intensity factor (SIF) was not taken into account in the analysis.

(a) General view

(b) Crack-tip coordinates and crack propagation angle
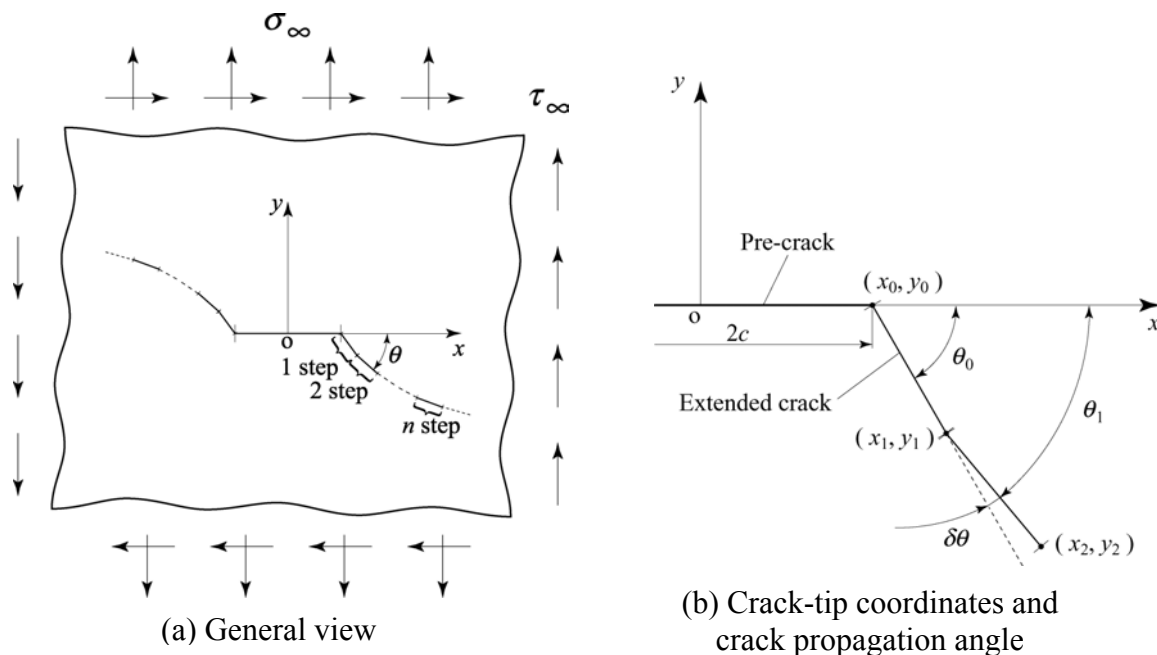
Figure 1. Model for crack propagation in infinite plate under tensile and shear stress.

Crack Propagation Criterion

Consider a crack whose tip is located at (x_1, y_1) as shown in Fig. 1(b). The tangential stress range σ_θ near the crack tip was calculated from the stress intensity factor for mode I, K_I, and for mode II, K_{II}, of the crack by

$$\sigma_\theta = \frac{K_I}{\sqrt{2\pi r}} \cos^3\left(\frac{\delta\theta}{2}\right) - 3\frac{K_{II}}{\sqrt{2\pi r}} \cos^2\left(\frac{\delta\theta}{2}\right) \sin\left(\frac{\delta\theta}{2}\right) \tag{1}$$

where $\delta\theta$ is the change of the angle of crack extension from the current crack direction and r is the distance from the current crack tip. The direction of the maximum tangential stress direction is given by

$$\tan\left(\frac{\delta\theta}{2}\right) = \frac{1}{4}\frac{K_I}{K_{II}} - \frac{1}{4}\sqrt{\left(\frac{K_I}{K_{II}}\right)^2 + 8} \tag{2}$$

The variation of σ_θ in one cycle is calculated from loading conditions. Three versions of the maximum tangential stress criterion are used for prediction of fatigue crack propagation.

(1) $\Delta\sigma_{\theta max}$ criterion: This $\Delta\sigma_{\theta\,max}$ criterion assumes the direction of crack extension coincident with the direction perpendicular to the maximum of the total range of the tangential stress including the negative stress at the crack tip. The crack closure is neglected.

(2) $\Delta\sigma^+_{\theta\,max}$ criterion: For fatigue crack propagation, only the tensile part of the cyclic stress can be effective. The $\Delta\sigma^+_{\theta\,max}$ criterion assumes the direction of crack propagation coincident with the direction perpendicular to the maximum of the positive range of tangential stress at the crack tip.

(3) $\Delta\sigma^*_{\theta\,max}$ criterion: Under reverse loading, crack surfaces may come into contact with each other. By taking into account of crack-face contact and neglecting the frictional force, the minimum value of SIF was calculated by BFM and is denoted by K^*_{min}. For closed cracks, the mode II component K^*_{IImin} is not zero, while $K^*_{Imin} = 0$. The range of the tangential stress and the crack direction are calculated by substituting the ranges of stress intensity factors, ΔK_I^* and ΔK_{II}^*, for K_I and K_{II} in Eqs (1) and (2).

Simulation of Crack Propagation

The simulation of fatigue crack propagation was conducted through step-by-step process. Figure 1(b) illustrates a crack propagated from a precrack by one step. The crack tip is now located at point (x_1, y_1) and the angle of the crack with respect to the precrack is θ_1. The SIF values of K_I and K_{II} were first calculated by BFM. The direction of crack propagation $\delta\theta$ is determined from the three criteria described above. The deviation of the crack propagation direction is caused by the mode II stress intensity factor, and the crack propagates straight under pure mode I loading. The amount of crack extension for one step is determined by

$$\Delta c = (dc/dN) \times N \tag{3}$$

where $N = 1000$ cycles. The value of dc/dN (m/cycle) is the power function of the maximum stress intensity factor k_{Imax} (MPa) for a medium-carbon steel as

$$dc/dN = C\left(k_{\mathrm{Imax}}\right)^{m} \tag{4}$$

where $C = 1.76 \times 10^{-12}$ and $m = 3.69$ [9]. The k_{Imax} value for an extended crack by Δc from the existing crack is equal to

$$k_{\mathrm{Imax}} = \sigma_{\theta}\sqrt{2\pi r} = K_{\mathrm{Imax}}\cos^{3}\left(\frac{\delta\theta}{2}\right) - 3K_{\mathrm{IImax}}\cos^{2}\left(\frac{\delta\theta}{2}\right)\sin\left(\frac{\delta\theta}{2}\right) \tag{5}$$

where $\delta\theta$ is the angle of crack extension with respect to the current crack determined by Eq. (2), and K_{Imax} and K_{IImax} are the SIF values for the current crack at the maximum stress.

The crack propagation is simulated by repeating the above procedure. In the present simulation, the amount of crack extension by one step was about 10 μm at the beginning and then became larger with crack propagation.

EXPERIMENTAL PROCEDURE

Material and Specimen
A tubular specimen with the outer diameter of 16 mm and the inner diameter of 14 mm was made of a medium-carbon steel (JIS S45C). The chemical composition of the material was as follows (mass%) : C0.43, Si0.19, Mn0.81, P0.022, Cu0.01, Ni0.02, Cr0.14. After machining, the specimens were annealed at 1123 K for 1 hr. The yield strength was 319 MPa, the tensile strength was 583 MPa, Young's modulus was 216 GPa, and Poisson's ratio was 0.279 [4,5]. For notched specimens, a hole of diameter of 1 mm was introduced. For precracked specimens, a hole with the diameter of 0.2 mm was first introduced at the center of the specimens, and the specimens were precracked under cyclic axial tension-compression. The total length of the precrack was 1 mm. All the precracked specimens were stress-relieved at 923 K for 1 hr before fatigue testing.

Fatigue Testing
Fatigue tests were conducted in a computer-controlled electro-servo hydraulic tension-torsion fatigue testing machine (Shimadzu EHF-ED10 /TQ-40L). The loading conditions were five cases:
(1) Case A: Cyclic torsional stress at the stress ratio $R = -1$, torsional stress amplitude $\tau_{\mathrm{a}} = 100$ MPa.
(2) Case B: Cyclic torsional stress at $R = -1$ with superposition of a static tension, $\sigma_{\mathrm{m}} = 100$ MPa, equal to the torsional stress amplitude, $\tau_{\mathrm{a}} = 100$ MPa.
(3) Case C: Cyclic torsional stress at $R = -1$ with superposition of a in-phase cyclic axial stress amplitude, $\sigma_{\mathrm{a}} = 100$ MPa, equal to the torsional stress amplitude, $\tau_{\mathrm{a}} = 100$ MPa.
(4) Case D: Cyclic tension compression of the amplitude $\sigma_{\mathrm{a}} = 100$ MPa at $R = -1$.
(5) Case E: Cyclic tension compression of the amplitude $\sigma_{\mathrm{a}} = 100$ MPa at $R = -1$, with superposition of static torsional stress of the magnitude 100 MPa.

The crack propagation direction and the crack propagation rate were determined from plastic replicas taken from the specimens. Replicas were examined with a

scanning electron microscope after coating gold. A digital microscope was also used for monitoring crack extension from a precrack.

NOTCH EFFECT ON FATIGUE CRACK PROPAGATION

Prediction of Crack Initiation Site
When tensile and shear stresses, σ and τ, are applied to a plate with a hole as shown in Fig. 2(a), the tangential stress, $\bar{\sigma}_\theta$, around the circumference is expressed as

$$\bar{\sigma}_\theta = \sigma + 2\sigma \cos 2\theta - 4\tau \sin 2\theta \qquad (6)$$

The tangential stress, σ_θ, calculated from the nominal stresses as shown in Fig. 2(b) is

$$\sigma_\theta = \frac{\sigma}{2} + \frac{\sigma}{2}\cos 2\theta - \tau \sin 2\theta \qquad (7)$$

From Eqs. (6) and (7), we have

$$\bar{\sigma}_\theta = 4\sigma_\theta - \sigma \qquad (8)$$

The angle where the tangential stress on the hole circumference takes the maximum is coincident with the maximum tangential stress of the nominal stress.

On the circumference of the hole, the stress state is uniaxial and fatigue cracks are expected to initiate at the angle where the range of the tangential stress takes the maximum. Those angles are $\pm 45^\circ$ and $\pm 135^\circ$ for cases A and B, and -31.7° and -148.3° for case C. For case D, the angles are 0° and 180°.

Prediction of Crack Propagation Path
An infinite plate with a hole of 1 mm diameter is subjected to uniform tensile and shear stresses as shown in Fig. 3. For each case of loading, a crack of 20 μm in length is located at the site of crack initiation determined from the criterion described in the preceding section, and subsequent propagation is predicted based on the three criteria. Four cracks are formed for cases A and B, while two cracks for case C.

(a) Stress field   (b) Nominal stress field
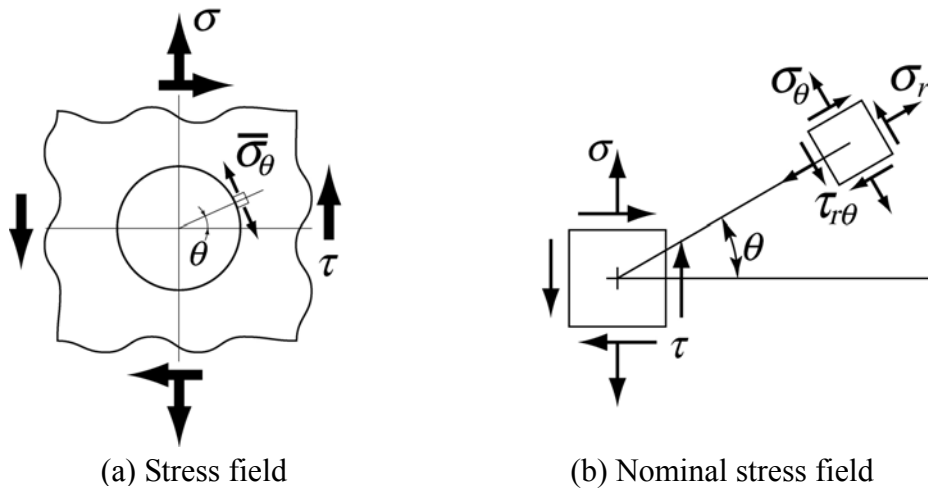
Figure 2. Stress field in specimen with a hole and cracks.
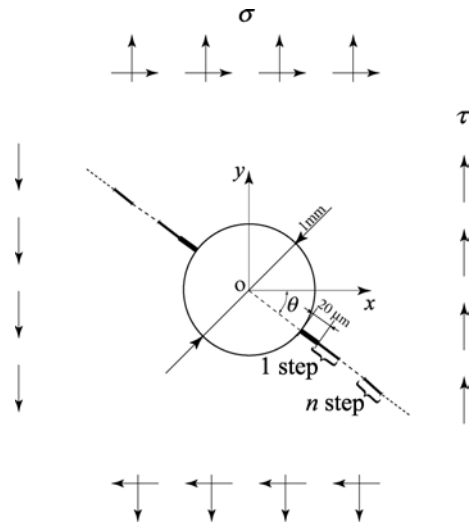
Figure 3. Model for crack propagation from a hole in infinite plate.

(a) Case A

(b) Case B

Case C

$\Delta\sigma_{\theta\max}$ criterion

$\Delta\sigma^{*}_{\theta\max}$ criterion
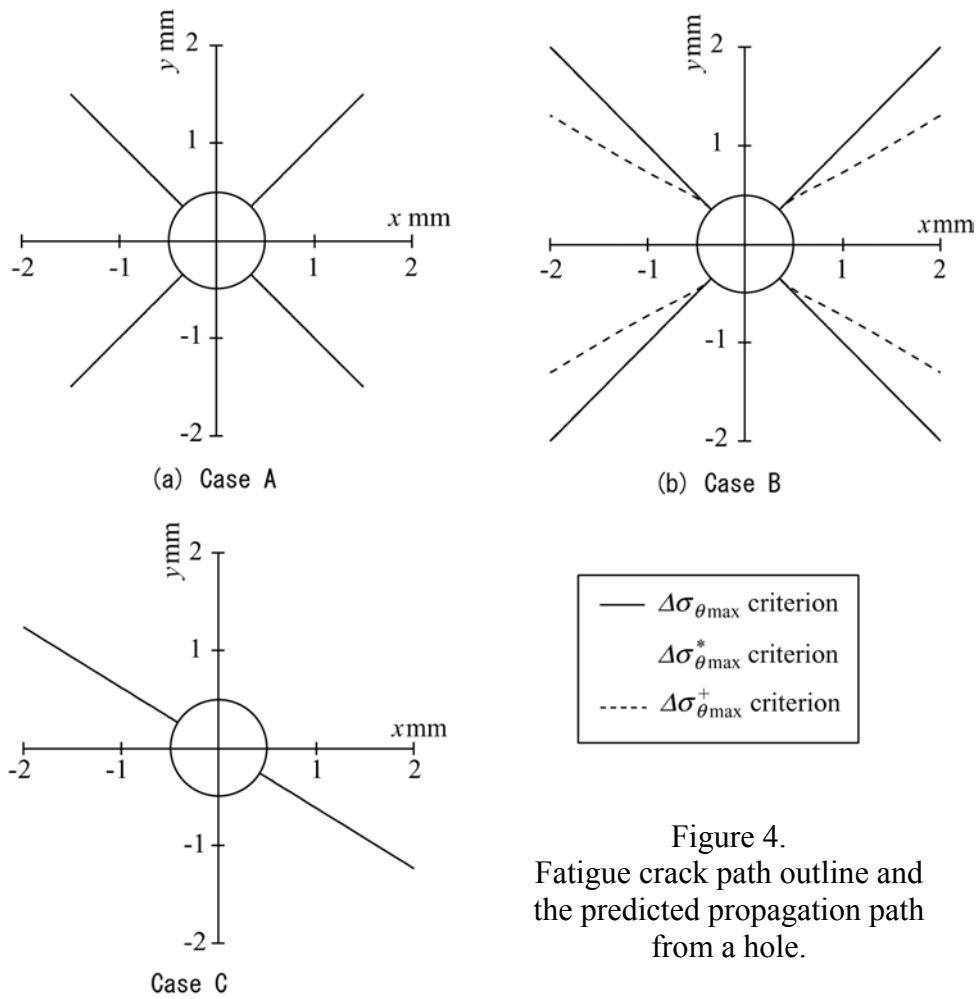
$\Delta\sigma^{+}_{\theta\max}$ criterion

Figure 4.
Fatigue crack path outline and the predicted propagation path from a hole.

Figure 4 shows the results. For cases A and C, the three criteria predict the identical crack path which is shown with the solid line. For case C, the $\Delta\sigma_{\theta\mathrm{max}}$ and $\Delta\sigma^*_{\theta\mathrm{max}}$ criteria give the identical path, while the $\Delta\sigma^+_{\theta\mathrm{max}}$ criterion gives a different path which is shown with the dotted line. For all cases, fatigue cracks propagate straight.

On the basis of the nominal stresses, we assume criterion I giving the crack direction perpendicular to the maximum range of the tangential stress, and criterion II giving that perpendicular to the maximum of the positive range of the tangential stress. The crack paths predicted based on criteria I and II are identical to those based on the $\Delta\sigma_{\theta\mathrm{max}}$ (or $\Delta\sigma^*_{\theta\mathrm{max}}$) criterion and the $\Delta\sigma^+_{\theta\mathrm{max}}$ criterion, respectively.

Comparison with Experiments

Figure 5 are the micrographs of cracks observed for cases A, B and C [10]. Table I shows the experimental and predicted angles of cracks. For case B, the experimental angle agrees well with the prediction based on based on the $\Delta\sigma_{\theta\mathrm{max}}$ (or $\Delta\sigma^*_{\theta\mathrm{max}}$) criterion and criterion I.

(a) Case A
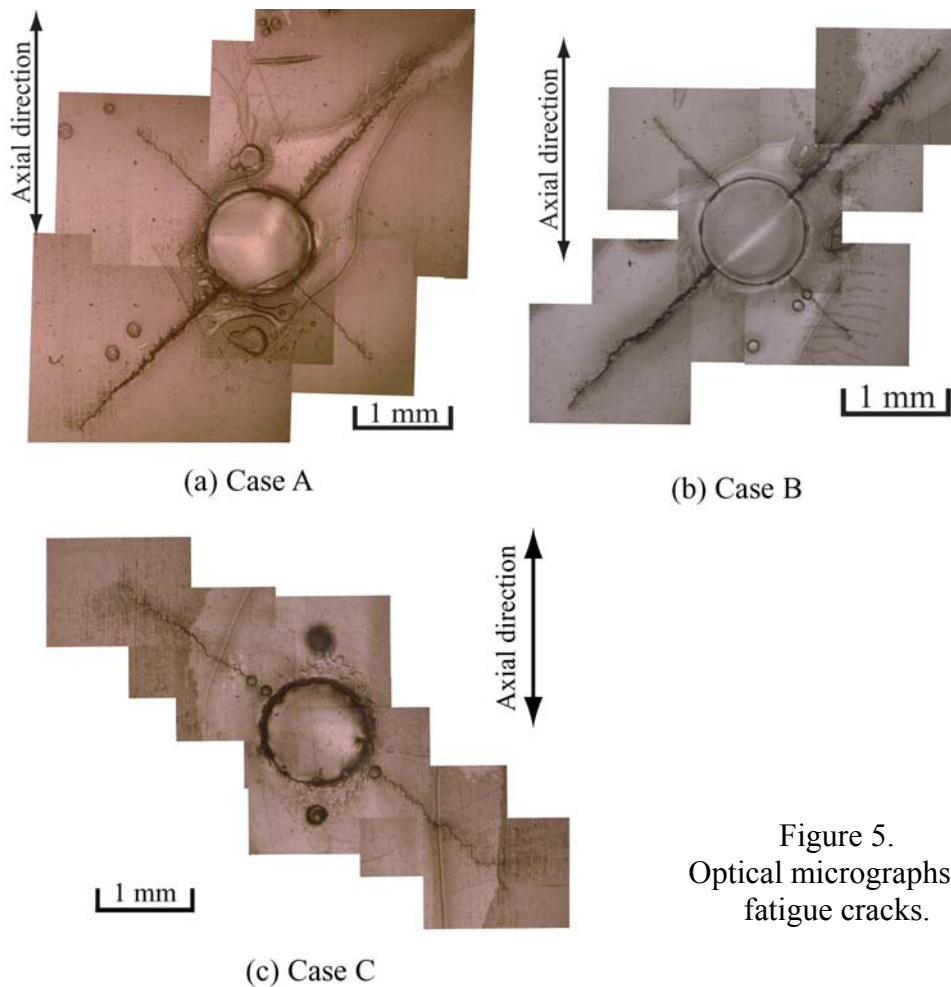
(b) Case B

(c) Case C

Figure 5.
Optical micrographs of fatigue cracks.

Table 1. Crack propagation angles (deg).

Crack	Case A			Case B			Case C		
No.	(i)	(ii)	(iii)	(i)	(ii)	(iii)	(i)	(ii)	(iii)
1	45.1	45	45	49	45	32	-	58.3	58.3
2	-46.5	-45	-45	-46	-45	-32	-35.5	-31.7	-31.7
3	-133	-135	-135	-137	-135	-148	-	-121.7	-121.7
4	138	135	135	134	135	148	142	148.3	148.3

(i) Experimental data,　(ii) Prediction $\Delta\sigma_{\theta max}$, $\Delta\sigma_{\theta max}^{*}$ and criterion I
(iii) Prediction $\Delta\sigma_{\theta max}^{+}$ and criterion II.

LOAD-VARIATION EFFECT ON FATIGUE CRACK PROPAGATION

Prediction of Crack Path

The effect of combined mode loading on the propagation path of a mode I precrack made by axial loading was studied in our previous paper. The propagation path was predictable based on the $\Delta\sigma_{\theta max}$ and $\Delta\sigma^{*}_{\theta max}$ criteria.　It was concluded that the crack path was controlled by the alternating range of the stress, and not influenced by the superposed mean stress. This is true, even when there is crack closure.　The crack deviation is caused by the existence of the mode II stress intensity range, $\Delta K_{II}{}^{*}$, and the crack propagation direction given by the $\Delta\sigma_{\theta max}$ (or $\Delta\sigma^{*}_{\theta max}$) criterion is nearly identical to the direction with $\Delta K_{II}{}^{*} = 0$.

So far the fiction coefficient is assumed to be 0 in the prediction.　Assuming the frictional coefficient is 0.5, the crack path from an inclined crack is predicted. Since the

(a) Initial crack angle = -45°　　　(b) Initial crack angle = -31.7°
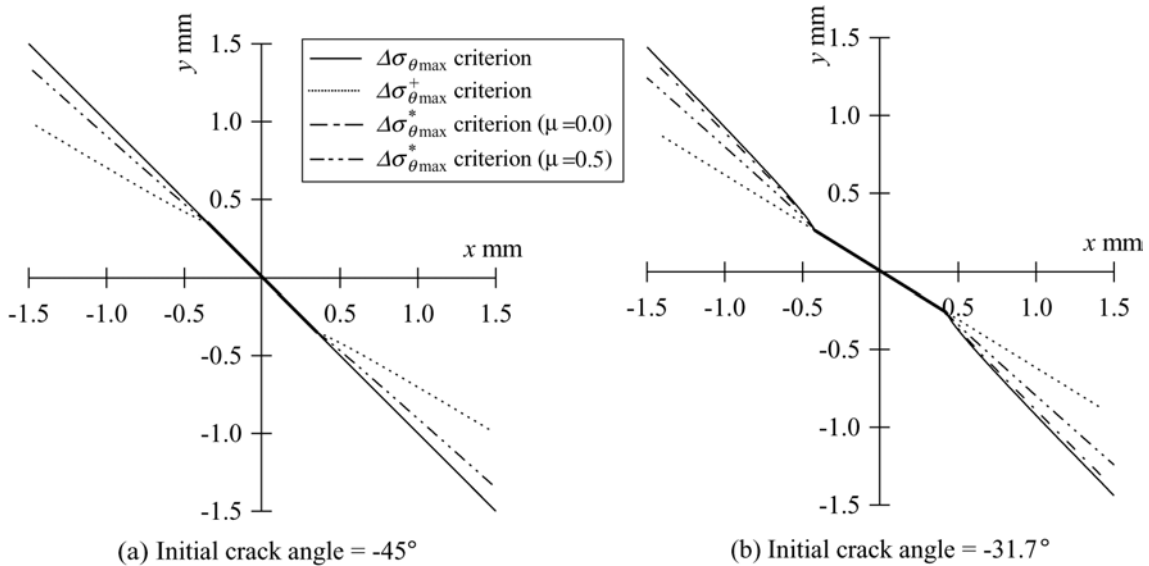
Figure 6. Effect of friction in crack-face contact on the
predicted crack path from an inclined pre-crack.

difference in the crack path is predicted only for case B, the crack propagation simulation from a precrack inclined -45° or -31.7° under loading case B. Figure 6 shows the prediction. The crack path for small fictional coefficient is close to the prediction by the $\Delta\sigma_{\theta max}$ criterion and that for larger coefficient is closer to the prediction by the $\Delta\sigma^{+}_{\theta max}$ criterion.

Comparison with Experiments

A precrack of about 1 mm in length was introduced under loading case A and then the specimen was stress relieved at 923 K. The crack propagation under loading case B is shown in Fig. 7(a), where the tips of precracks are indicated. Cracks propagate form 45° precracks without changing crack directions. Figure 7(b) show the influence of subsequent case B loading on the propagation path from precracks formed with -31.7° under loading case C. Precracks with -31.7° angle deviated to -45° under case B loading. From these two examples, it can be concluded that the crack path in predictable based on the $\Delta\sigma_{\theta max}$ or $\Delta\sigma^{*}_{\theta max}$ criterion even when there is crack closure.
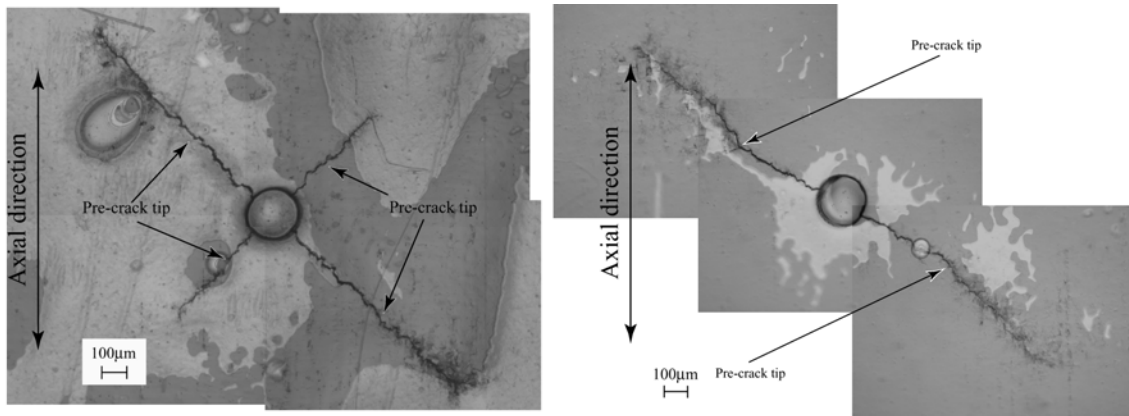
(a) Initial crack angle = -45° made under case A

(a) Initial crack angle = -32° made under case C

Figure 7. Optical micrographs of fatigue cracks for case B.

EFFECT OF STATIC MODE II ON FATIGUE CRACK PROPAGATION

Effect of Static Shear Mode on Crack Propagation

In our simulation model, the superposition of static mode II loading on cyclic mode I loading does not have any influence on the propagation path of cracks if the crack is straight. Real cracks show some deviation of the crack path by the superposed static mode II or shear loading. Figure 8 shows an example of cracks propagating for case E. The precrack propagated under cyclic axial stress amplitude of 100 MPa with $R = -1$ by 0.3 mm, and a static negative shear stress τ_m = -100 MPa was superposed for crack extensions from 0.3 to 0.8 mm, and then a positive stress τ_m = 100 MPa was superposed
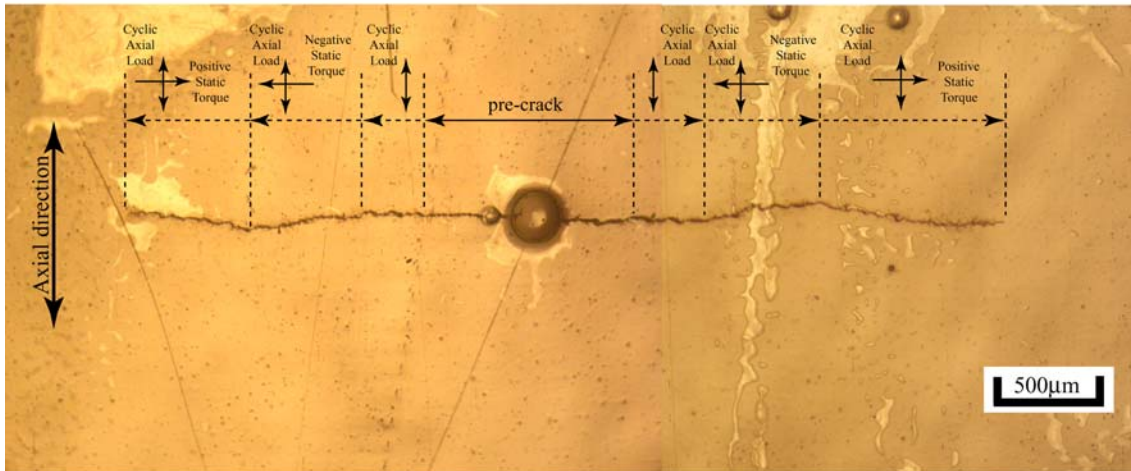
Figure 8. Fatigue crack propagation from a pre-crack under $\tau_m=\pm100$MPa or 0 MPa, $\sigma_a=100$MPa, $R=-1$, $N=2.06 \sim 10^6$ (Case E).

for crack extension from 0.8 to 1.3 mm. Small amount of deviation was observed when static shear stress was superposed and the direction is reversed by reversing the static shear direction. This deviation may be caused by the crack shape which is not straight, but zigzag. Even when the applied stress is macroscopically mode I, static shear stress gives rise to the contact of crack faces, and then induces the cyclic component of mode II loading at the crack tip.
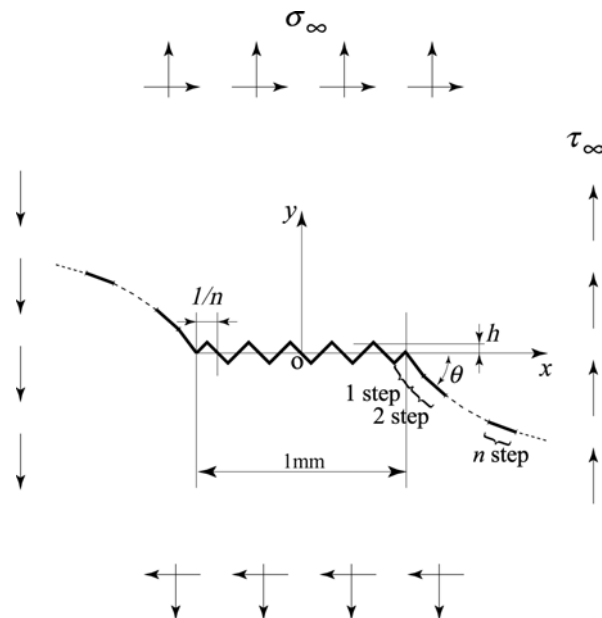
Figure 9. Model for crack propagation from a zigzag pre-crack in infinite plate under tensile and shear stress.

Prediction of Crack Path and Comparison with Experiments

Figure 9 shows a mode I crack with zigzag shape and the total length of the crack is 1 mm. The propagation of the crack under case E loading is simulated using the $\Delta\sigma^{*}_{\theta\max}$ criterion.

Figure 10 shows the crack path on the left side of cracks which have initially the number of zigzags $n = 10$, 20, and 30, and the height of $h = 10$, 15, and 20 μm.   The solid line is the outline of the experimentally observed cracks. The number of hills is more influential to crack deviation than the hill height. The experimental path is most close to the path predicted for the case of $n = 10$ and $h = 15$ mm.
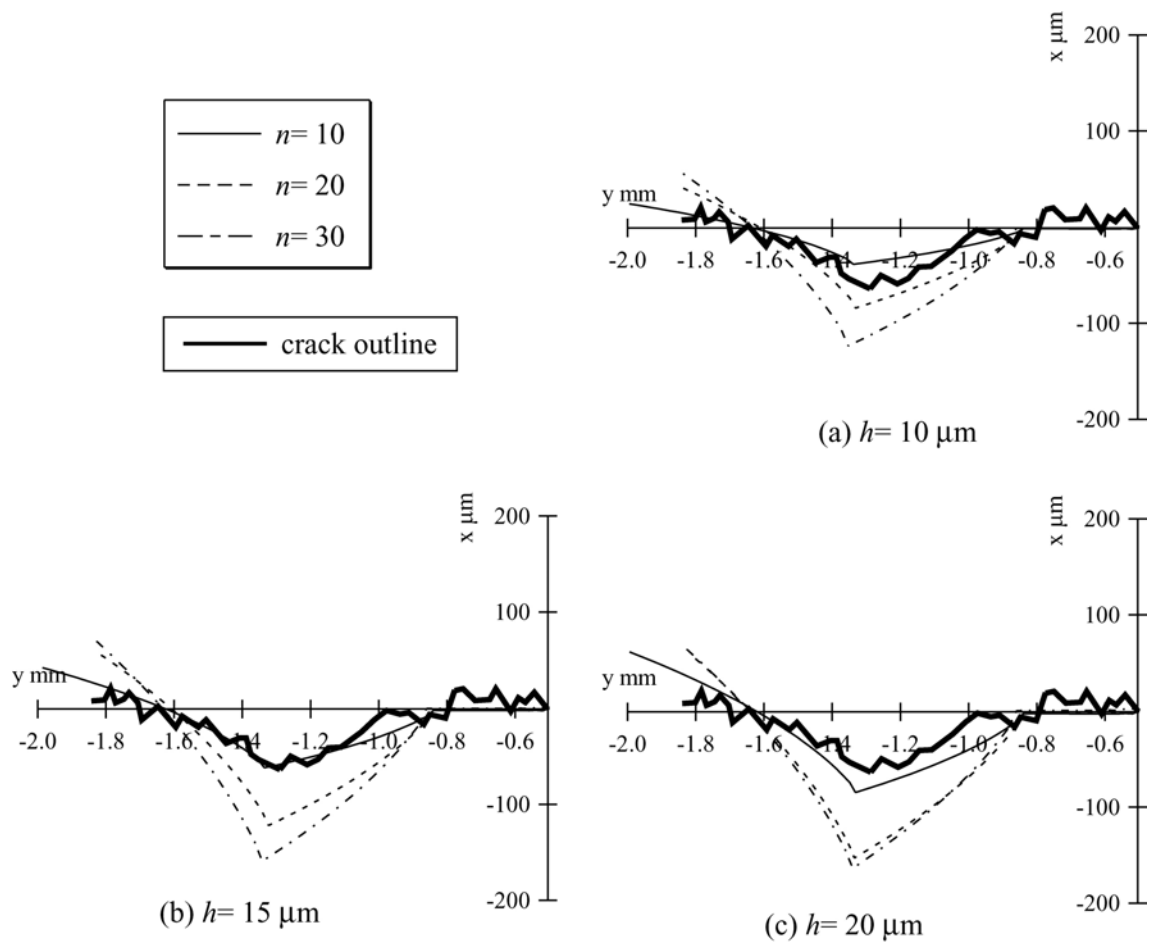
Figure10. Fatigue crack path and the predicted crack path of Case E (left).

CONCLUSIONS

A simulation of fatigue crack propagation from a hole or crack under combined axial and torsional loading was conducted on the basis of the maximum tangential stress criterion for determining the crack path. The simulation results of the crack propagation path were compared with the experimental results obtained from fatigue tests by using thin-walled tubular specimens made of a medium-carbon steel.

(1) Fatigue cracks were nucleated at the position of the maximum of the amplitude of the tangential stress around the hole, and propagated straight away from the hole.

(2) The path of fatigue crack propagation from a hole or a crack followed the direction perpendicular to the maximum of the range of the tangential stress, $\Delta\sigma^{*}_{\theta\max}$, near the crack tip calculated from the stress intensity ranges by considering the contact of crack faces near the minimum load.

(3) The mode II stress intensity factor range was responsible for crack deviation. It quickly became close to zero after small amount of crack extension.

(4) The crack path predicted from the $\Delta\sigma^{*}_{\theta\max}$ criterion was very close to that calculated from the maximum of the total range of the tangential stress, $\Delta\sigma_{\theta\max}$, calculated by neglecting the crack face contact.

(5) The superposition of static mode II shear loading changes slightly the propagation path of a crack propagating under axial tension compression. This deviation was caused by the generation of cyclic mode II component due to the zigzag shape of a fatigue crack.

REFERENCES

[1] Erdogan, F ., Sih, G.C. (1963) *J. Basic Eng.,* **85**, 519-527.

[2] Richard, H., Linnig, W., Henn, K.(1991) *Forensic Eng.,* **3**, 99-109.

[4] Tanaka, K., Akiniwa, Y., Kato, T, Mikuriya, T. (2003) *Fatigue Fract. Engng Mater. Struct.,* 28, 73-82.

[5] Tanaka, K., Akiniwa, Y., Kato, T, Takahashi, H. (2005) *Trans. Jpn Soci. Mech. Engrs,* **A 71,** 607-614.

[6] Nisitani, H. (1978), In: *Mechanics of Fracture*, Vol. 5, pp. 1-68, Sih, G. C. (Ed.), Noordhoff Inter. Publ.

[7] Kitagawa, H., Yuuki, R., Tohgo, K. (1981) *Trans. Jpn Soci. Mech. Engrs,* **A 47,** 1283-1292.

[8] Sumi, Y., (1985) *Theor. Appl. Fract. Mech.,* **4,** 149-156.

[9] Zhang, L. M., Akiniwa, Y., Tanaka, K., (1998) *Trans. Jpn Soci. Mech. Engrs,* **A 64**, 1229-1235.

[10] Tanaka, K., Akiniwa, Y., Takahashi, A., Mikuriya, T., (2003) *Trans. Jpn Soci. Mech. Engrs,* **A 69,** 1001-1008.